# A Measurement Technique for Infrared Emissivity of Epoxy-Based Microwave Absorbing Materials

Derek A. Houtz, *Member, IEEE*, and Dazhen Gu, *Senior Member, IEEE*

***Abstract*— Infrared (IR) emissivity is a critical parameter for modeling and predicting heat transfer by radiation. Microwave absorbing materials, having a high emissivity in the microwave spectrum, are crucial in a wide array of applications, such as electromagnetic interference mitigation, stealth technology, and microwave remote sensing and radiometer calibration. Accurate knowledge of the thermal properties of these materials is necessary for efficient design and optimization of these types of systems. Typical microwave absorbing materials consist of a dielectric epoxy material impregnated with a lossy material, such as iron or carbon. We study a novel cryogenically compatible epoxy-based absorber material that has been loaded with varying concentrations of carbonyl iron powder (CIP). We study six materials with CIP concentrations of 0%, 5%, 10%, 20%, 30%, and 50% by tap volume. We use a commercial IR camera with sensitivity in the range 7.5–13 $\mu$m to measure the radiance of the samples and a waterbath IR blackbody at ten temperatures between about 19 °C and 45 °C. A linear Deming fitting is performed, considering uncertainties in both the measured parameters, and the slope of the linear fit is shown to be the IR emissivity, averaged over the spectral response of the camera. The emissivity ranges between 0.868 and 0.757, decreasing monotonically as a function of iron carbonyl concentration between 0% and 50%. The uncertainty of the emissivity determination method is derived and presented. The uncertainty of the presented method is shown to be no larger than 3.3% for all measured samples.**

***Index Terms*— Emissivity measurement, heat transfer, infrared (IR) emissivity, microwave absorber, microwave blackbody, radiometer calibration, thermal properties.**

## I. Introduction

THERMAL infrared (IR) emissivity is a simple scalar quantity often used in heat transfer and thermodynamics applications to quantify heat transfer by radiation. Knowledge of a material's IR emissivity is a prerequisite to thermal system design and modeling, particularly when predicting the temperature of a body. The coupling between thermal and microwave behavior is of importance for passive microwave remote-sensing calibration, because microwave brightness temperature is a function of a body's physical temperature [1]. Characterization of calibration blackbodies in microwave remote sensing requires knowledge of their physical temperature [2], [3]. Design and characterization analyses of passive microwave calibration sources use thermal models to predict their physical temperature [4]–[6], which requires accurate knowledge of the thermal properties of the chosen materials [7]. The physical temperature of a blackbody's surface is a function of thermal IR emissivity and can result in additional calibration uncertainty if not accurately known [8]. According to Planck's law of radiation, at temperatures between 19 °C and 45 °C, the vast majority of radiated power is in the IR regime with no more than $10^{-6}$% radiating at other wavelengths.

Thermal behavior of microwave absorbing materials is also of interest in the fields of radar stealth technology [9], electromagnetic interference mitigation [10], and biotechnology [11].

Many of the methods currently in the literature for determining IR emissivity with an IR camera lack a rigorous uncertainty analysis [12], neglect reflections, and are only accurate for high values of emissivity with bodies above ambient temperatures [13]. The method used in this letter improves on the established two-temperature method [14], because it does not depend on the absolute calibration accuracy of the IR camera and uses more than two temperature points to reduce random statistical errors.

The material studied in this letter was recently developed and has been used in microwave and millimeter wave radiometer calibration sources such as those discussed in [15] and [16]. The material uses a cryogenically compatible epoxy that is intended to have a similar coefficient of thermal expansion to metals. The material is loaded with carbonyl iron powder (CIP) of various concentrations to tune its complex permittivity and permeability in the microwave regime, thus controlling its microwave absorbing properties. We investigate CIP concentrations ranging from 0% to 50%, above which the material begins to lose mechanical stability. In this letter, we determine this material's thermal IR emissivity and whether CIP concentration influences thermal IR emissivity.

In Section II, we discuss the theoretical approach to the emissivity measurements. In Section III, we discuss the experimental setup. Section IV presents the results and provides some brief discussion of the findings. Finally, Section V draws conclusions from this letter.

## II. Theoretical Approach

Emissivity describes the radiant energy emitted from a body, compared with an ideal blackbody at the same temperature. Emissivity can be wavelength-dependent, called spectral emissivity, or can be taken as an average over a spectral response across a specific bandwidth. We are concerned with the whole thermal IR spectrum and use a sensor that has sensitivity across this band from 7.5 to 13 $\mu$m. The spectrally averaged

Manuscript received October 5, 2017; revised November 1, 2017; accepted November 8, 2017. Date of publication December 4, 2017; date of current version December 27, 2017. This work was supported by the U.S. Government. *(Corresponding author: Derek A. Houtz.)*

The authors are with the RF Technology Division, National Institute of Standards and Technology, Boulder, CO 80305 USA (e-mail: derek.houtz@nist.gov; dazhen.gu@nist.gov).

Color versions of one or more of the figures in this letter are available online at http://ieeexplore.ieee.org.

Digital Object Identifier 10.1109/LGRS.2017.2772783

emissivity can be expressed as [17]

$$\varepsilon = \frac{\int_{\lambda_1}^{\lambda_2} s(\lambda) L_{\text{emit}}(\lambda, T) d\lambda}{\int_{\lambda_1}^{\lambda_2} s(\lambda) L_{\text{BB}}(\lambda, T) d\lambda} = \frac{R_{\text{emit}}(T)}{R_{\text{BB}}(T)} \tag{1}$$

where $\varepsilon$ is the spectrally averaged emissivity, $s(\lambda)$ is the spectral response function of the detector, $L_{\text{emit}}$ is the spectral exitance of the true surface, $L_{\text{BB}}$ is the spectral radiance of a blackbody as described by Planck's law of radiation, $\lambda_1$ and $\lambda_2$ are wavelength endpoints of detector sensitivity, $R_{\text{emit}}$ is the spectrally averaged emitted radiance from the surface, and $R_{\text{BB}}$ is the spectrally averaged blackbody radiance. The term $R_{\text{emit}}$ is typically not directly measurable, because in real-world situations, there is also a radiance contribution from reflected radiation from the background and from the detector itself. The spectrally averaged radiance measured by an IR detector can be expressed as

$$R_{\text{meas}}(T) = R_{\text{emit}}(T) + R_{\text{refl}} \tag{2}$$

where $R_{\text{meas}}$ is the radiance of a true object measured by an IR detector, and $R_{\text{refl}}$ is the contribution of reflections to the measured radiance. We assume that $R_{\text{refl}}$ is independent of the sample temperature, a constant dependent only on the background environment. We also assume a constant detector temperature. By solving (2) for $R_{\text{emit}}$, substituting into (1), and rearranging, we arrive at the expression

$$R_{\text{meas}}(T) = R_{\text{BB}}(T')\varepsilon + R_{\text{refl}} \tag{3}$$

which is a linear combination, in slope-intercept form, of measurable parameters and the desired quantity, emissivity. By measuring both the radiance of an IR blackbody and the radiance of the sample of interest at multiple temperatures, we can perform a linear fit to obtain the desired emissivity and, incidentally, also quantify the reflected radiance. The $T'$ in (3) refers to the fact that the equilibrium temperatures for the blackbody and sample are slightly different for the same water circulator set-temperatures due to differences in heat transfer coefficients. To correct for this offset, the blackbody radiance is interpolated to the sample temperatures by the usage of interpolation along a fourth-order polynomial fit. This form is chosen, because the relationship is expected to approximately follow the Stefan–Boltzmann law. After this offset correction, we have a set of ten pairs of $R_{\text{meas}}$ and $R_{\text{BB}}$ at the same temperatures to be fit to (3). At extreme temperatures, the IR emissivity may no longer be independent of temperature and (3) would no longer be valid.

Traditional least squares linear fitting only considers possible errors in one dependent variable. In our case, both parameters $R_{\text{meas}}$ and $R_{\text{BB}}$ are measured values with associated measurement errors. We use the Deming method [18], a special case of the total least squares method, for the linear fit of the two uncertain parameters. The standard error of the slope from this linear fitting gives type A uncertainty $u_{\varepsilon,\text{Type A}}$ also known as the statistical or random error. We use the jackknife method [18] to estimate type A uncertainty as

$$u_{\varepsilon,\text{Type A}} = \sqrt{\frac{n-1}{n}\sum_{i=1}^{n}\left(\tilde{\varepsilon}_i - \bar{\tilde{\varepsilon}}\right)^2} \tag{4}$$

where $n$ is the number of observations ($n = 10$ in our case), $\tilde{\varepsilon}_i$ refers to the Deming fit emissivity calculated by omitting the $i$th observation, and $\bar{\tilde{\varepsilon}}$ refers to the mean of the $n$ calculated $\tilde{\varepsilon}_i$ values.

Type B or systematic uncertainty $u_{\varepsilon,\text{Type B}}$ is derived from the manufacturer specification of the IR sensor and the calibration accuracy of the radiance measurements. A differential uncertainty analysis [19] results in

$$u_{\varepsilon,\text{Type B}} = \sqrt{\left(\frac{\partial\varepsilon}{\partial R_{\text{meas}}} u_{R_{\text{meas}}}\right)^2 + \left(\frac{\partial\varepsilon}{\partial R_{\text{BB}}} u_{R_{\text{BB}}}\right)^2} \tag{5}$$

where $u_{R_{\text{meas}}}$ is the radiance measurement uncertainty in the commercial IR camera, $u_{R_{\text{BB}}}$ is the combined blackbody radiance measurement uncertainty, considering contributions from the nonideality of the IR blackbody and from the temperature interpolation error and is given by

$$u_{R_{\text{BB}}} = \sqrt{u_{R_{\text{meas}}}^2 + [(1-\varepsilon_{\text{BB}}) * R_{\text{BB}}]^2 + \text{MSE}_{\text{int}}} \tag{6}$$

where $\varepsilon_{\text{BB}}$ refers to the emissivity of the blackbody and $\text{MSE}_{\text{int}}$ is the mean-squared error of the blackbody radiances relative to the fourth-order polynomial fit of sample temperatures versus measured radiances. The second term under the radical in (6) results from the nonideal IR emissivity of the blackbody. As discussed in Section III, $\varepsilon_{\text{BB}}$ is taken here as 0.995, the "worst case" value. Because of the small relative contribution of the nonideal emissivity in our case, we take this to be a Gaussian distributed error. The usage of a lower emissivity blackbody, or higher uncertainty of this emissivity, could result in a negative bias of the resulting sample emissivity.

The partial derivatives in (5) are calculated by solving (3) for emissivity and differentiating. The partial derivatives, or sensitivity terms, depend on the measured radiance values. We use the lowest temperature measurement, which results in the highest sensitivity and thus the worst case uncertainty value. The total uncertainty in the derived emissivity is calculated from the root squared sum of type A and type B uncertainties

$$u_\varepsilon = \sqrt{u_{\varepsilon,\text{Type A}}^2 + u_{\varepsilon,\text{Type B}}^2} \tag{7}$$

where $u_\varepsilon$ is the overall uncertainty in the emissivity from this method. Section III discusses how the radiance quantities are experimentally measured.

## III. Experimental Setup

A set of epoxy-based material samples of varying iron carbonyl powder concentrations by volume were cast into waveguide shims for characterization of their microwave material properties, as discussed in [15]. The same samples are used in this study, in which we investigate the thermal IR emissivity of the materials. The samples are 10.7 mm by 4.3 mm and about 2.5 mm thick. The samples are fastened to a temperature-controlled brass plate. The temperature of the plate is controlled with a water circulator of nominal temperature stability ±0.01 °C. A calibrated platinum resistance thermometer (PRT) is attached to the back side of the plate

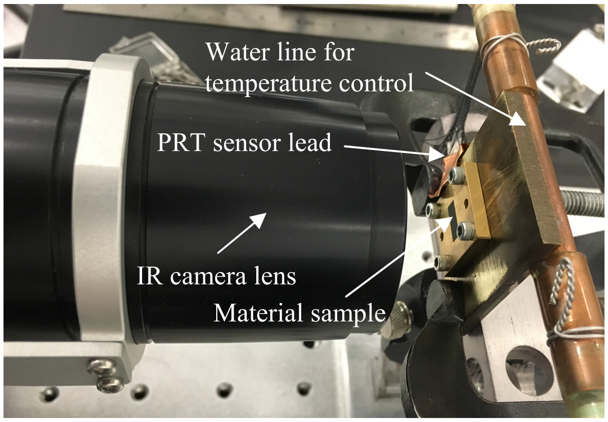


Fig. 1. Photograph of experimental setup for sample measurements.

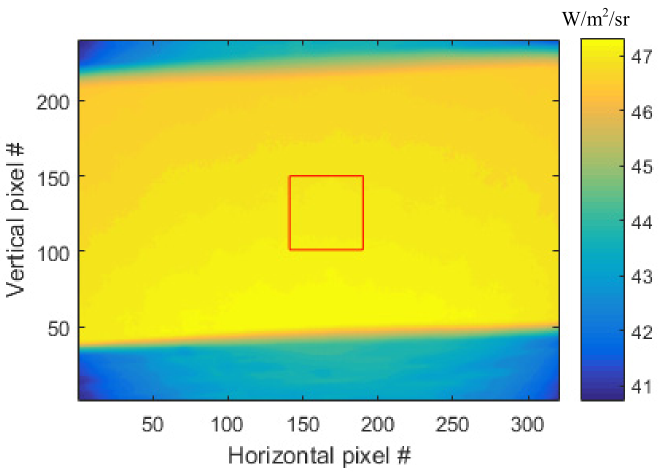


Fig. 2. Example of measured sample IR radiance image. The shown image is of the pure epoxy sample at a set temperature of 45 °C. The red box encloses the pixels used in the averaging.

with thermal paste and a copper tape to monitor the physical temperature of the sample.

We use a commercial thermal IR camera to view the samples with a close-up lens. The lens has a field of view of 6 mm by 8 mm with a resolution of 25 $\mu$m per pixel at a focal distance of 2 cm. Fig. 1 shows the camera viewing the sample attached to the brass plate.

The set-temperature of the water circulator is varied to ten temperatures ranging between 19 °C and 45 °C, while the temperature of the sample is monitored and the radiance is measured. These temperatures were chosen to provide a range of radiances while maintaining negligible temperature gradients between the PRT measured temperature and the radiating surface of the sample. We captured ten calibrated images of the sample at each set temperature and analyzed a small square of 50 by 50 pixels near the center of the sample. The mean radiance over this subset of the image is taken and also averaged over the ten images. Fig. 2 shows an example of the image taken of the sample for the unloaded epoxy at 45 °C.

A conical water-bath IR blackbody known as CASOTS [20] was measured to obtain the $R_{\mathrm{BB}}$ radiance values. The CASOTS blackbody has been shown to have comparable performance to a National Institute of Standards and Technology

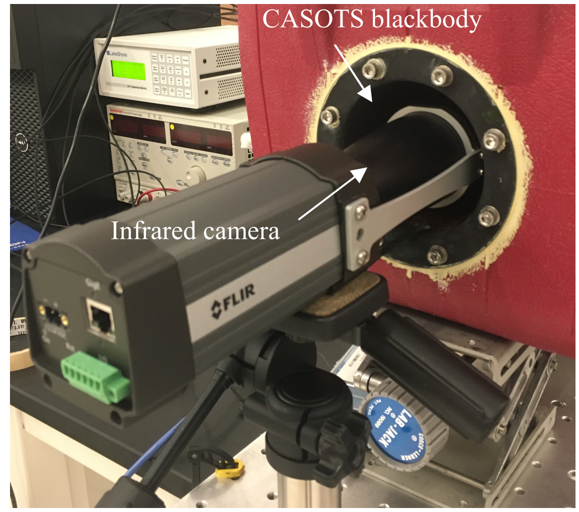


Fig. 3. Experimental setup for blackbody measurement. The IR camera looking into the CASOTS IR blackbody is shown.

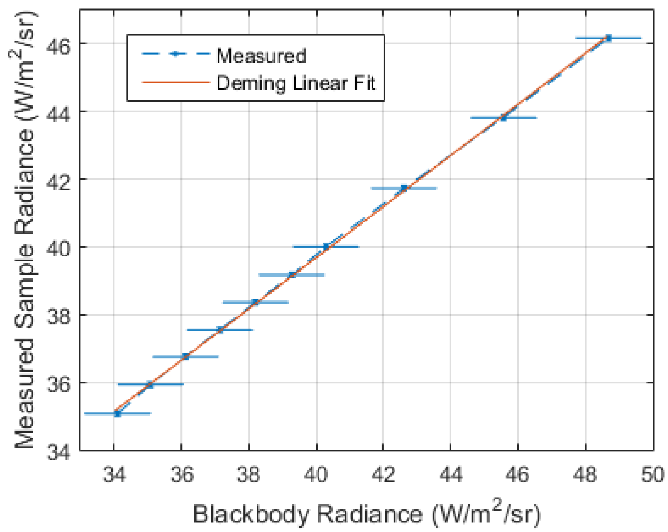


Fig. 4. Blue dashed line shows the measured IR radiance of the 50% CIP sample versus the measured blackbody radiance along with error bars in both the axes. Error bars are plotted as one standard uncertainty on either side of the data points. The red line shows the result of the Deming linear fit.

IR blackbody with IR emissivity of no less than 0.995 [20]. The same PRT sensor was attached to the blackbody cavity surface in the same way it was attached to the backside of the temperature-controlled brass sample holder. The temperature of the blackbody was controlled with the same refrigerating–heating water circulator used for the samples and is set to the same ten temperatures. As stated previously, the same circulator set-temperatures result in slightly different equilibrium temperatures of the samples and blackbody due to their different emissivities and convective heat transfer coefficients. The averaging technique for the blackbody measurements is also identical to that of the sample measurements. The experimental setup with the camera looking into the conical blackbody is shown in Fig. 3.

## IV. Results and Discussion

The emissivity values and associated uncertainties for the six samples are calculated according to the method discussed

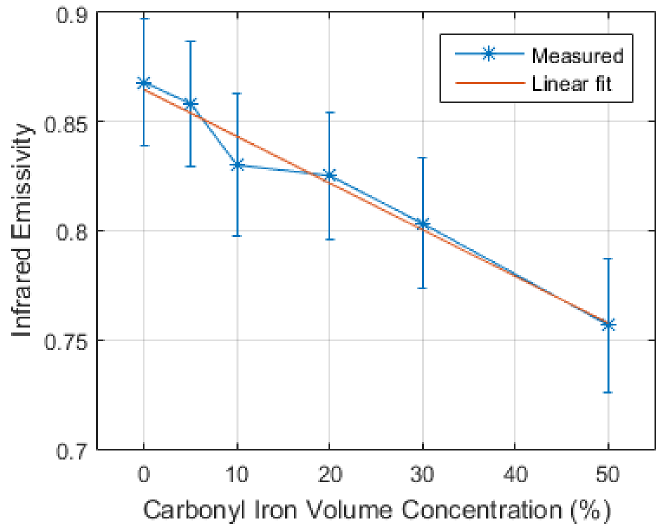


Fig. 5. Thermal IR emissivity of the epoxy-based microwave absorber material as a function of CIP loading concentration in percent tap volume. The blue line shows the measured data and the red line provides a linear fit of the data. Error bars are plotted as one standard uncertainty on either side of the data points.

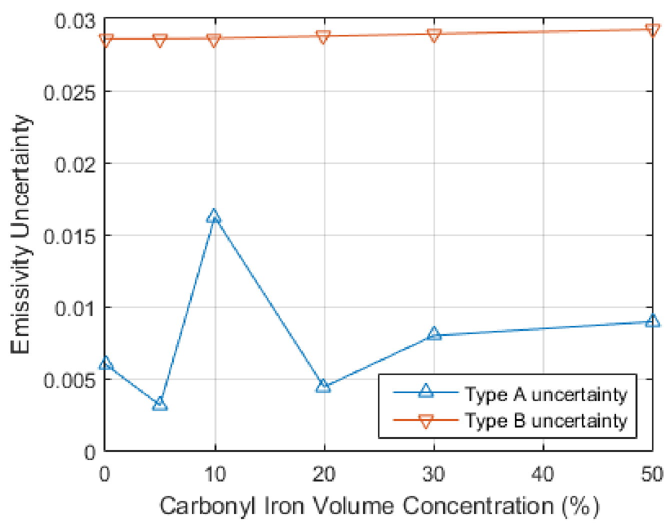


Fig. 6. Uncertainty contributions in thermal IR emissivity of epoxy-based microwave absorber material as a function of CIP loading concentration in percent tap volume.

in Section II. An example of the measured data and linear fit of (3) is shown in Fig. 4 for the 50% CIP sample. The calculated emissivity values and uncertainty error bars are shown in Fig. 5. We see a significant decrease in IR emissivity as a function of iron carbonyl loading percentage. This is expected as the IR emissivity of pure iron is lower than that of epoxy. The monotonically decreasing trend appears to be approximately linear, allowing us to define a linear relationship between emissivity and CIP loading percentage. Optimization of the microwave properties of absorber materials often involves tuning the CIP loading percentage, so we can define the following empirical equation to determine the thermal IR emissivity for arbitrary loading percentage:

$$\varepsilon = 0.87 - 0.0021 * \%\mathrm{CIP} \tag{8}$$

where %CIP is the concentration of CIP loading in percent by tap volume. The result at 10% CIP appears to deviate slightly from the linear trend of the remaining points. We believe that this is due to procedural error of not allowing the sample to fully thermally stabilize at one or multiple temperature points, or a change in the reflected background temperature during the measurement. This procedural error results in an inflated type A uncertainty from the Deming fit, because these points do not fit the linear relationship of (3) as closely. The contributions from type A and type B uncertainties are shown in Fig. 6 as a function of CIP loading percent.

## V. Conclusion

We have demonstrated a simple yet effective method for measuring spectrally averaged thermal IR emissivity along with associated measurement uncertainty using an affordable commercial thermal imaging system. We provide measured emissivity results and uncertainties for a suite of newly developed microwave absorber materials and also provide a generalized formula for determining the emissivity of a material with an arbitrary concentration of CIP loading. We found that CIP loading does significantly alter the thermal emissivity, causing a monotonic decrease in emissivity with CIP loading.

CIP loaded epoxy absorbers are widely used in microwave radiometer calibration sources in which both the microwave performance and thermal IR performance are of great importance. The results presented here will allow precise modeling, design, and simulation of present and future calibration sources, leading to improved brightness temperature accuracy and precision. Other industries may also benefit from the results presented here including biomedical, defense, and consumer electronics.

## References


[1] E. M. Twarog, W. E. Purdy, P. W. Gaiser, K. H. Cheung, and B. E. Kelm, "WindSat on-orbit warm load calibration," *IEEE Trans. Geosci. Remote Sens.*, vol. 44, no. 3, pp. 516–529, Mar. 2006.

[2] D. A. Houtz and D. K. Walker, "A finite element thermal simulation of a microwave blackbody calibration target," in *Proc. IEEE Int. Geosci. Remote Sens. Symp. (IGARSS)*, Melbourne, VIC, Australia, Jul. 2013, pp. 394–397.

[3] A. Murk, A. Schröder, M. Winser, Y. Qian, and R. Wylde, "Temperature/absorption cross integrals and the validation of radiometric temperatures for space-based radiometers," in *Proc. 10th Eur. Conf. Antennas Propag. (EuCAP)*, Davos, Switzerland, Apr. 2016, pp. 1–3.

[4] S. Fernandez, A. Murk, and N. Kämpfer, "Design and characterization of a peltier-cold calibration target for a 110-GHz radiometer," *IEEE Trans. Geosci. Remote Sens.*, vol. 53, no. 1, pp. 344–351, Jan. 2015.

[5] D. W. Draper, D. A. Newell, D. A. Teusch, and P. K. Yoho, "Global precipitation measurement microwave imager prelaunch hot load calibration," *IEEE Trans. Geosci. Remote Sens.*, vol. 51, no. 9, pp. 4731–4742, Sep. 2013.

[6] A. Murk *et al.*, "Low mass calibration target for MM-wave remote sensing instruments," *IEEE Trans. Antennas Propag.*, vol. 61, no. 4, pp. 1547–1556, Apr. 2013.

[7] I. Zivkovic and A. Murk, "Boron nitride loading for thermal conductivity improvement of composite microwave absorbers," *Electron. Lett.*, vol. 48, no. 18, pp. 1130–1131, Aug. 2012.

[8] D. A. Houtz, "NIST microwave blackbody: The design, testing, and verification of a conical brightness temperature source," Ph.D. dissertation, Dept. Aerosp. Eng. Sci., Univ. Colorado, Boulder, CO, USA, 2017.

[9] Y. P. Chen, G. Y. Xu, T. C. Guo, and N. Zhou, "Infrared emissivity and microwave absorbing property of epoxy-polyurethane/annealed carbonyl iron composites coatings," *Sci. China Technol. Sci.*, vol. 55, no. 3, pp. 623–628, Mar. 2012.

[10] J. Zhou *et al.*, "Direct incorporation of magnetic constituents within ordered mesoporous carbon-silica nanocomposites for highly efficient electromagnetic wave absorbers," *J. Phys. Chem. C*, vol. 114, pp. 7611–7617, Mar. 2010.

[11] D. Diaz-Bleis, C. Vales-Pinzón, Y. Freile-Pelegrin, and J. J. Alvarado-Gil, “Thermal characterization of magnetically aligned carbonyl iron/agar composites,” *Carbohydrate Polymers*, vol. 99, pp. 84–90, Jan. 2014.

[12] *Standard Test Methods for Measuring and Compensating for Emissivity Using Infrared Imaging Radiometers*, Standard ASTM E1933-97, American Society Testing Materials, Pennsylvania, PA, USA, 1997.

[13] *User's Manual FLIR A3xx pt Series*, document T559795, FLIR Syst. Inc., Wilsonville, OR, USA, ch. 16, accessed: Aug. 24 2017. [Online]. Available: http://flir.com/uploadedFiles/Security/Products/A-Series/a3xxPT-Series-Users-Manual.pdf

[14] R. P. Madding, “Emissivity measurement and temperature correction accuracy considerations,” *Proc. SPIE*, vol. 3700, pp. 393–401, Mar. 1999.

[15] D. A. Houtz *et al.*, “Electromagnetic design and performance of a conical microwave blackbody target for radiometer calibration,” *IEEE Trans. Geosci. Remote Sens.*, vol. 55, no. 8, pp. 4586–4596, Aug. 2017.

[16] K. Jacob, A. Schroder, M. Kotiranta, and A. Murk, “Design of the calibration target for SWI on JUICE,” in *Proc. 41st Int. Conf. Infr., Millim., Terahertz Waves (IRMMW-THz)*, Copenhagen, Denmark, Sep. 2016, pp. 1–2.

[17] T. Islam, G. C. Hulley, N. K. Malakar, R. G. Radocinski, P. C. Guillevic, and S. J. Hook, “A physics-based algorithm for the simultaneous retrieval of land surface temperature and emissivity from VIIRS thermal infrared data,” *IEEE Trans. Geosci. Remote Sens.*, vol. 55, no. 1, pp. 563–576, Jan. 2017.

[18] K. Linnet, “Estimation of the linear relationship between the measurements of two methods with proportional errors,” *Statist. Med.*, vol. 9, no. 12, pp. 1463–1473, Dec. 1990.

[19] *Guide to the Expression of Uncertainty in Measurement (GUM)*, document 100, International Bureau of Weights and Measures, Joint Committee for Guides in Metrology (JCGM), 2008.

[20] C. J. Donlon, T. Nightingale, L. Fiedler, G. Fisher, D. Baldwin, and I. S. Robinson, “The calibration and intercalibration of sea-going infrared radiometer systems using a low cost blackbody cavity,” *J. Atmos. Ocean. Tech.*, vol. 16, no. 9, pp. 1183–1197, Sep. 1999.